Supporting Information for Manuscript entitled "*Swarming in Shallow Waters*" by Siowling Soh[1], Michal Branicki[1] and Bartosz A. Grzybowski[1,2]*
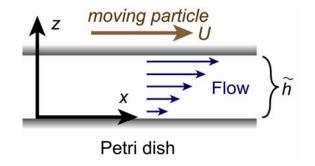
[1]Department of Chemical and Biological Engineering, Northwestern University, 2145 Sheridan Road, Tech E-136, Evanston, IL 60208

[2]Department of Chemistry, Northwestern University, 2145 Sheridan Road, Evanston, IL 60208

*To whom correspondence should be addressed:
E-mail: grzybor@northwestern.edu Phone: 847-491-3024

1. Drag force between bottom surface of a particle and the surface of the Petri dish

As narrated in the main text, for sufficiently thin water layers ($h < 1.4$ mm), there is little, if any, motion of the particles, even though they are not in contact with the base of the Petri dish (height of particles is 1 mm). This "stalling" can be rationalized by considering the drag exerted on the bottom of the boat by a thin layer (thickness $\tilde{h}$, Figure S1) of fluid separating it from the surface of the dish.

Figure S1. Scheme illustrating the velocity profile within the thin fluid layer between the bottom surface of the particle and the surface of the Petri dish.

Specifically, approximating the flow as a simple unidirectional flow between a moving plate (bottom surface of the particle) and a stationary plate (Petri dish; Figure S1), the Navier-Stokes equations reduce to $\dfrac{d^2 v_x}{dz^2} = \dfrac{1}{\mu}\dfrac{dP}{dx}$, where v_x denotes horizontal velocity, μ is viscosity and P is pressure. Assuming that the pressure drop is constant (which is exactly true for flow between infinite plates) and together with the boundary conditions, $v_x = U$ at $z = \tilde{h}$ and $v_x = 0$ at $z = 0$, this equation is easily solved to give $v_x = \dfrac{1}{2\mu}\dfrac{dP}{dx}\left(z - \tilde{h}\right)z 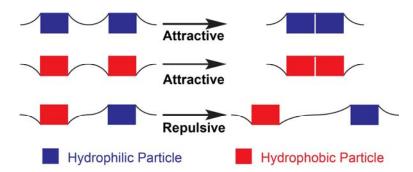+ \dfrac{U}{\tilde{h}}z$. The drag force acting on the bottom of the particle is obtained by evaluating: $F_D = \mu \left.\dfrac{\partial v_x}{\partial z}\right|_{\tilde{h}} A_{bottom}$, where A_{bottom} is the surface area of the bottom of the particle. Substituting for v_x gives $F_D = \left(\dfrac{1}{2}\dfrac{dP}{dx}\tilde{h} + \dfrac{\mu U}{\tilde{h}}\right)A_{bottom}$. For small $\tilde{h}$, this expression is approximately $F_D \approx \mu U A_{bottom}/\tilde{h}$, giving the scaling relationship $F_D \sim 1/\tilde{h}$. In other words, the drag force resisting particle's motion due to surface-tension effects becomes increasingly important as $\tilde{h}$ decreases. We note that the above analysis, in which the particle's bottom is assumed to be parallel to the surface of the dish, does not take into account the stability of such a configuration. Additional effects may become important in a more realistic case when the angle of inclination with respect to the bottom of the dish is allowed to vary. More detailed discussion of these effects can be found in, for example, Ref. S1.

2. Potential influence of capillarity.

In principle, attraction between the particles could be caused by capillary interactions due to the menisci forming between the particles[S2,S3] or by buoyancy effects which prevail over the "capillary suction" for sufficiently small particles.[S4] However, direct imaging of the interface (along it plane, using high-resolution camera) shows no appreciable menisci around the particles in either deep or shallow waters. Most importantly, we performed experiments in which either hydrophobic or hydrophilic particles (not soaked with camphor) were placed at the interface along with the camphor-soaked boats. If capillarity were at play, one type of these particles should be attracted to the boats, and the other, repelled (Figure S2). In reality, both types of particles are drawn toward the boats by the surface-tension-driven flows.

Figure S2. Illustrations of capillary forces acting between hydrophilic and hydrophobic particles. If the particles are of the same "type," (i.e., hydrophilic-hydrophilic or hydrophobic-hydrophobic), the particles attract one another. However, if the particles are of different "types" (i.e., hydrophobic-hydrophilic), the particles repel.

3. Estimation of the rate of sublimation, k

As camphor spreads on the interface around the particles, it also sublimates. The rate of sublimation, k, can be estimated experimentally from the time needed to sublimate all the camphor initially stored in the gel particle. In a typical experimental setup, a cylindrical gel particle (1 mm in diameter, 0.5 mm thick) was placed in a Petri dish (12 cm diameter), where motion of the particle normally persists for $t_{expt} \sim 2$ hours. Prior to use, the particle was soaked in a saturated solution of camphor-in-methanol for several hours. Since the mass of agarose in the particle was only 5%, the volume of methanol contained in the gel was close to the volume of the particle ($\sim 4 \times 10^{-10}$ m^3). The amount of camphor, m_c, stored in the gel can be calculated from the saturated concentration of camphor in methanol (1.1 g/mL) giving 10^{-4} g or 10^{-7} mol (molecular weight of camphor is 152 g/mol).

Knowing the amount of camphor initially stored in the gel particle, it is possible to calculate the flux, f, (with units mol/m^2·s) of camphor onto the interface for the total duration of $t_{expt} \sim 2$ hours. The area of the air-water interface is $A_I = 10^{-2}$ m^2 for a dish of 12 cm in diameter. The flux can be estimated using $f \sim m_c / \left(A_I \times t_{expt} \right)$, giving $f \sim 10^{-9}$ mol/ m^2·s.

This flux is related to k by assuming a first-order rate of sublimation as mentioned in the main text : $f = -kc_S$, where c_S is the concentration of camphor at the interface. Since spreading of camphor is strongly aided by convection, we assume here that the concentration of camphor in water is near saturation at 8 mM (verified later by concentration profiles from simulation). This means that $f \sim -kc_{Saturation}$, where the rate of sublimation is estimated to be $k \sim 10^{-10}$ m/s.

Supporting Information References:

S1.   Michell, A. G. M. Lubrication: Its Principles and Practice; Blackie and Son Ltd: London,

1950.

S2.   Bowden, N.; Terfort, A.; Carbeck, J.; Whitesides, G. M. Self-Assembly of Mesoscale

Objects into Ordered Two-Dimensional Arrays. Science **1997,** *276*, 233-235.

S3.   Grzybowski, B. A.; Bowden, N.; Arias, F.; Yang, H.; Whitesides, G. M. Modeling of

Menisci and Capillary Forces from the Millimeter to the Micrometer Size Range. *J. Phys.*

Chem. B **2001,** *105*, 404-412.

S4.   Vella, D.; Mahadevan, L. The "Cheerios Effect". *Am. J. Phys.* **2005,** *73*, 817-825.

Movie Legends:

Movie 1. Dynamic self-assembly of nine rod-shaped particles. These particles experience attractive force at large interparticle separations and repulsive force at short interparticle separations.

Movie 2. The assembly rotates when particles of different shapes and low symmetries are present. In this case, a small U-shaped particle is added to four rod-shaped particles.

Movie 3. Directional swarming of the assembly when a much larger particle with low symmetry is added to an ensemble of rod-shaped particles. Shown here is a large V-shaped particle together with six rod-shaped particles. The rod-shaped particles first assemble, then move behind the larger V-shaped "leader". Since the number of rod-shaped particle is even, the particles distribute themselves equally among the two arms of the large V-shaped particle, so that the swarm moves predominantly forward.

Movie 4. The assembly rotates when there is an odd number of rod-shaped particles (here, five) and a large V-shaped particle.

Movie 5. When the depth of the fluid is lowered further to ~ 1.6 mm, the assembly reversed its direction of motion as compared to Movie 3. In this case, the large V-shaped particle pushes six rod-shaped particles in front of the swarming assembly.

Movie 6. If the depth of the water layer is not uniform, they migrate toward shallow-water regions. In this video, the Petri dish has been tilted such that the water layer is shallower at the top than the bottom of the movie. In this case, the assembly moves upwards.

Movie 7. When there is a temperature gradient, the assembly also moves toward regions of higher temperature. In this movie, a copper wire is attached to a soldering iron. When the soldering iron is heated, the end of the copper wire not attached to the soldering iron is ~ 100 °C. The assembly is attracted to the copper wire and move toward it due to its high temperature.